MOLECULAR AND CELLULAR BIOLOGY, Apr. 1994, p. 2503–2515
0270-7306/94/$04.00+0

Vol. 14, No. 4

The *Aspergillus nidulans abaA* Gene Encodes a Transcriptional Activator That Acts as a Genetic Switch To Control Development

ALEX ANDRIANOPOULOS AND WILLIAM E. TIMBERLAKE*

Department of Genetics, University of Georgia, Athens, Georgia 30602

Received 22 October 1993/Returned for modification 9 December 1993/Accepted 12 January 1994

The *Aspergillus nidulans abaA* gene encodes a protein containing an ATTS DNA-binding motif and is required for the terminal stages of conidiophore development. Results from gel mobility shift and protection, missing-contact, and interference footprint assays showed that AbaA binds to the sequence 5′-CATTCY-3′, where Y is a pyrimidine, making both major- and minor-groove contacts. Multiple AbaA binding sites are present in the *cis*-acting regulatory regions of several developmentally controlled structural genes as well as those of the upstream regulatory gene *brlA*, the downstream regulatory gene *wetA*, and *abaA* itself. These *cis*-acting regulatory regions confer AbaA-dependent transcriptional activation in a heterologous *Saccharomyces cerevisiae* gene expression system. From these observations, we propose that the AbaA transcription factor establishes a novel set of feedback regulatory loops responsible for determination of conidiophore development.

Elucidation of the molecular mechanisms for developmental induction and determination is essential to our understanding of multicellular differentiation and organization. The signals, regulatory genes, and morphogenetic genes involved in these processes must be controlled temporally and spatially, and once triggered, a developmental fate should become determined at the appropriate stage to avoid the need for continued inductive signal. Sequential expression of three regulatory genes, *brlA*, *abaA*, and *wetA*, controls development of the asexual reproductive apparatus (conidiophore) of the filamentous fungus *Aspergillus nidulans* (18, 52). The *brlA* locus consists of overlapping transcription units, designated α and β, that encode functionally redundant proteins (42). *brlA*α encodes a C_2H_2 zinc finger protein (1) that has been implicated as a transcriptional activator by the results of expression studies in *Saccharomyces cerevisiae* (15). Forced expression of *brlA*α in *A. nidulans* vegetative cells under nonsporulating conditions induces transcription of numerous developmentally regulated structural genes as well as of the second regulatory gene in the pathway, *abaA*, and causes abnormal sporulation (1, 38). Forced expression of *abaA* under the same conditions also induces transcription of numerous developmentally regulated genes as well as of the third regulatory gene in the pathway, *wetA*, and of *brlA*α (38). However, forced *abaA* expression does not lead to spore formation, although it strongly inhibits growth and causes major morphological changes. The observation that *brlA*α induces *abaA* transcription and vice versa suggested that these two genes are linked in a positive feedback loop (38).

The predicted AbaA amino acid sequence contains the ATTS/TEA DNA-binding motif (5, 13), which is also present in the human transcription factor TEF-1 (56), the *Drosophila melanogaster* developmental regulator scalloped (14), and the *S. cerevisiae* Ty1 regulator *TEC1* (31). We tested the hypothesis that AbaA is a sequence-specific DNA-binding protein by assaying for its ability to bind to *cis*-acting regulatory sites identified upstream of the developmentally regulated *yA* gene by expression studies in *A. nidulans* and *S. cerevisiae* (8) and to upstream sequences from other, less well characterized structural and regulatory genes. The results presented in this article show that AbaA binds with high affinity and specificity to the sequence 5′-CATTCY-3′, where Y is a pyrimidine, and makes both major- and minor-groove contacts. Multiple AbaA binding sites are present upstream of the *wetA* and *brlA*α regulatory genes, suggesting that they are directly activated by *abaA*. Multiple AbaA binding sites are also present upstream of *abaA* itself. DNA fragments from *brlA*α, *abaA*, *wetA*, and two structural genes containing the AbaA binding sites mediated *abaA*-directed transcriptional activation in a heterologous *S. cerevisiae* expression system, indicating that the elements function in vivo.

These results support the model that after initial activation of *abaA* by *brlA*, AbaA activates the downstream regulatory gene *wetA* and serves as a positive-feedback regulator of itself and *brlA*. These positive-feedback loops are predicted to maintain the central regulatory pathway in the activated state, making continued development independent of the signals that initially triggered it. Therefore, *abaA* activation appears to act as a genetic switch to relieve the requirement for the primary exogenous cues responsible for developmental induction.

MATERIALS AND METHODS

Plasmids and DNA fragments. The *yA* promoter-derived sequences in pAA60 (−161 to −60) and pAA62 (−88 to −60) were obtained from plasmids pRA97 and pRA99 (8) and cloned into pBluescript II KS+ (Stratagene, Inc., La Jolla, Calif.) at the *Bam*HI site. The mutant *yA* promoter sequences were generated by using T4 DNA polymerase and previously described overlapping mutant oligonucleotides (8). The fragments were cloned into pBluescript II KS+ at the *Bam*HI site to yield pAA67, pAA69, pAA70, and pAA77.

Construction of expression and reporter plasmids. pAA37, containing the entire *abaA* coding region fused to the 3′ end of *Escherichia coli lacZ*, was constructed by ligating an intronless version of *abaA* (as an *Nco*I [end filled]-*Pst*I fragment) into the *Bam*HI (end filled)-*Pst*I sites of the pUR291 *lacZ* expression vector (43). The intronless version of *abaA* was generated by in

* Corresponding author. Present address: Myco Pharmaceuticals Inc., Building 300, One Kendall Square, Cambridge, MA 02137. Phone: (617) 374-9090. Fax: (617) 225-2997.

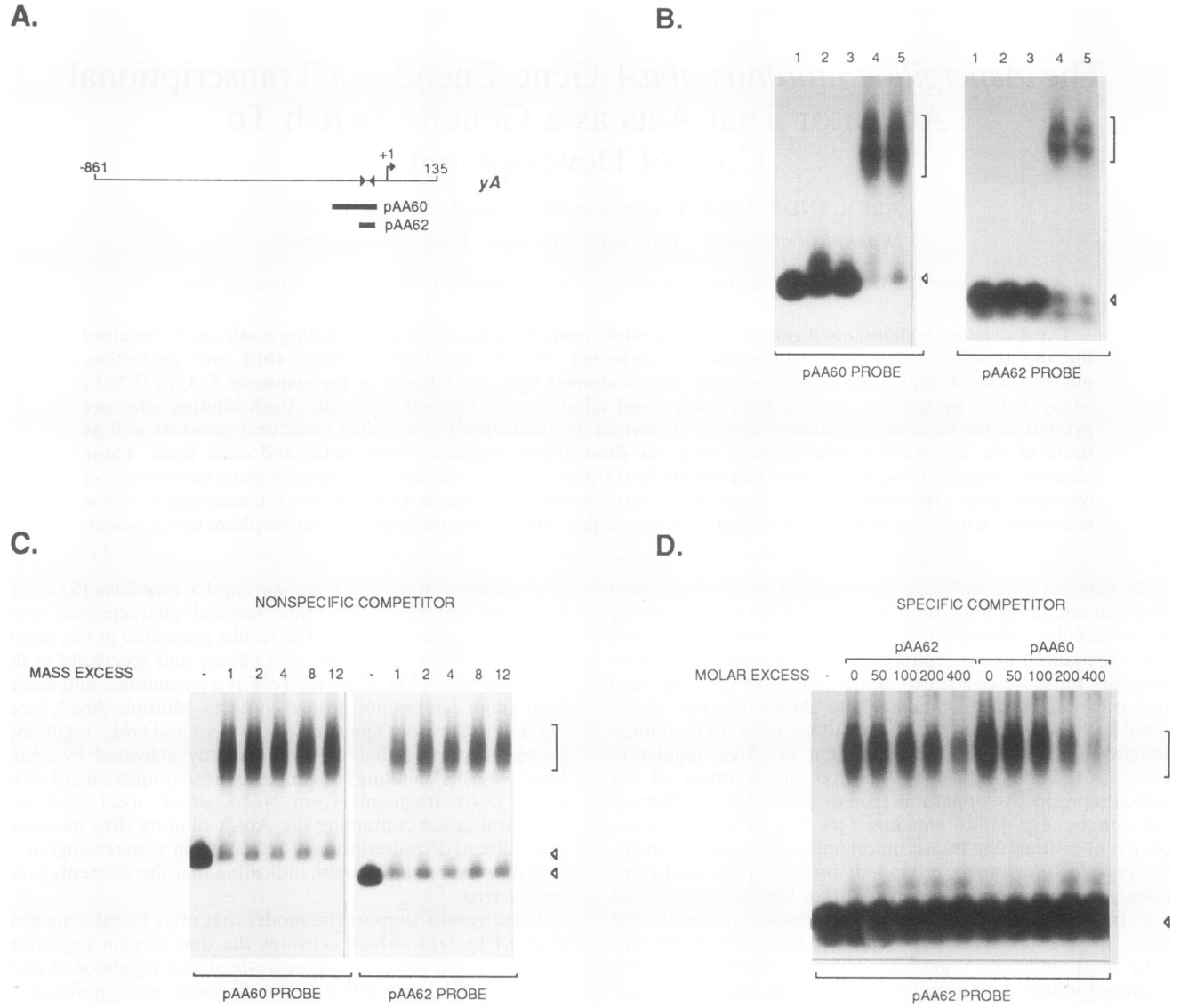

FIG. 1. Specific DNA binding of the LacZ-AbaA protein. (A) Mobility shift probes. The *yA* 5′ region is shown with the 5′ and 3′ coordinates, transcription initiation site (+1), putative AbaA binding sites (solid arrowheads), and the region spanned by the two probes (pAA60 and pAA62) used for the mobility shift analysis (thick line) indicated. (B) Mobility shift analysis with *yA* fragments containing putative AbaA binding sites. Protein extracts used were crude lysates from *E. coli* cells containing either pUR291 (control; lanes 2 and 3) or pAA37 (expressing LacZ-AbaA fusion product; lanes 4 and 5). The amount of protein added was 30 μg. Nonspecific competitor was poly(dI-dC) at 0 μg (lanes 2 and 4) or 4 μg (lanes 3 and 5). Lane 1 contained probe to which no protein extract was added. Bound probe (bracket) and unbound probe (open arrowhead) are indicated. (C) Nonspecific competition with the pAA60 and pAA62 probes. A mass excess of the nonspecific competitor poly(dI-dC) of 1×10^3 to 12×10^3, as shown above each lane, was used. AbaA protein was added as a crude *E. coli* lysate (30 μg) containing the LacZ-AbaA fusion product. Bound probe (bracket) and unbound probe (open arrowhead) are indicated. (D) Specific competition with the pAA62 probe and either pAA60 or pAA62 as a competitor. The molar excess of specific competitor is shown above each lane. Each reaction mix was supplemented with DNA from a plasmid similar in construction to pAA60 and pAA62 but lacking putative AbaA binding sites, so that the total molar excess of DNA was equal in all reactions. AbaA protein was added as a crude *E. coli* lysate (30 μg) containing the LacZ-AbaA fusion product. Bound probe (bracket) and unbound probe (open arrowhead) are indicated.

vitro mutagenesis (30) with oligonucleotides ABAIONE (5′-GATGCCTTCCAGCAAGCTCTTGAAGCAAACCC-3′) and ABAITWO (5′-GGGTGACCCTGATTGGGAGAGAC TTGTCCG-3′).

The *S. cerevisiae* expression plasmid pAA35 was constructed by fusing the intronless version of *abaA*, as an *Nco*I-*Eco*RI fragment, to the galactose-inducible *GAL1* promoter and untranslated leader at the translation initiation codon in the centromeric plasmid pAA54 (constructed from pRS313 [45] and pMTL [provided by C. N. Giroux]). pRS313 was digested with *Sac*I and *Nae*I, and the ends were blunted with mung bean nuclease and religated to remove *lacZ* sequences and part of the *fl* region. An *Xho*I (end filled)-*Sac*I fragment from this construct was replaced by a *Pvu*II-*Sca*I fragment from pBR322 to remove all *lacI* sequences. Finally, an *Eco*RI-*Sal*I fragment from pMTL, containing the *GAL1-GAL10* intragenic region, was inserted into the *Eco*RI-*Sal*I sites of the polylinker to yield pAA54. The *S. cerevisiae* reporter plasmids were constructed

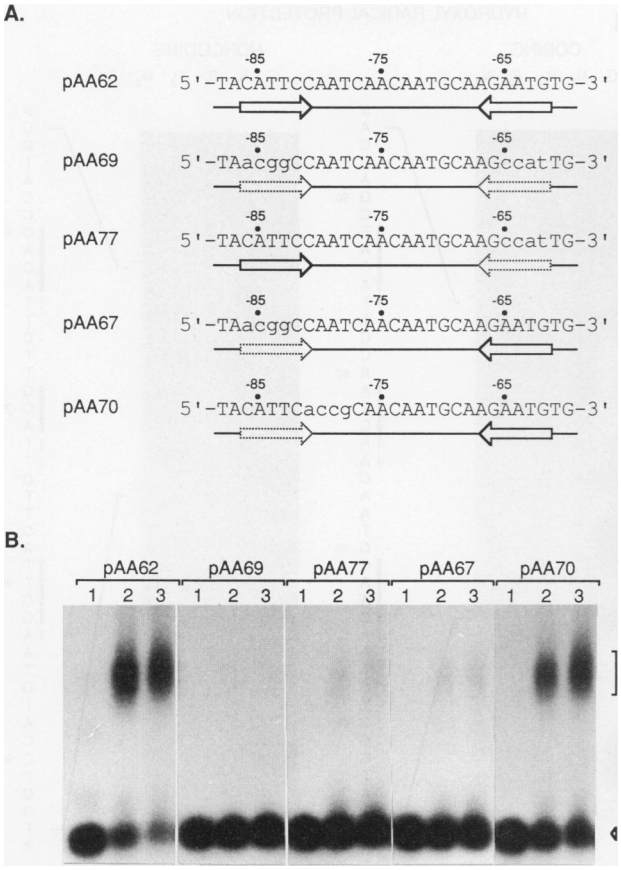

FIG. 2. Mutational analysis of AbaA binding sites. (A) Sequences of the wild-type and mutant AbaA binding sites. Lowercase letters indicate altered bases. Coordinates above each sequence are relative to the *yA* transcription initiation site. Solid-line arrows represent wild-type binding sites, whereas dotted-line arrows represent mutant sites. (B) Mobility shift analysis with the pAA62, pAA69, pAA77, pAA67, and pAA70 probes. The lanes in each probe set contained no added protein extract (lane 1), 5 μg of protein extract (lane 2), or 20 μg of protein extract (lane 3). The protein extract was cell lysate from *E. coli* cells containing pAA37, expressing the LacZ-AbaA fusion product. Bound probe (bracket) and unbound probe (open arrowhead) are indicated.

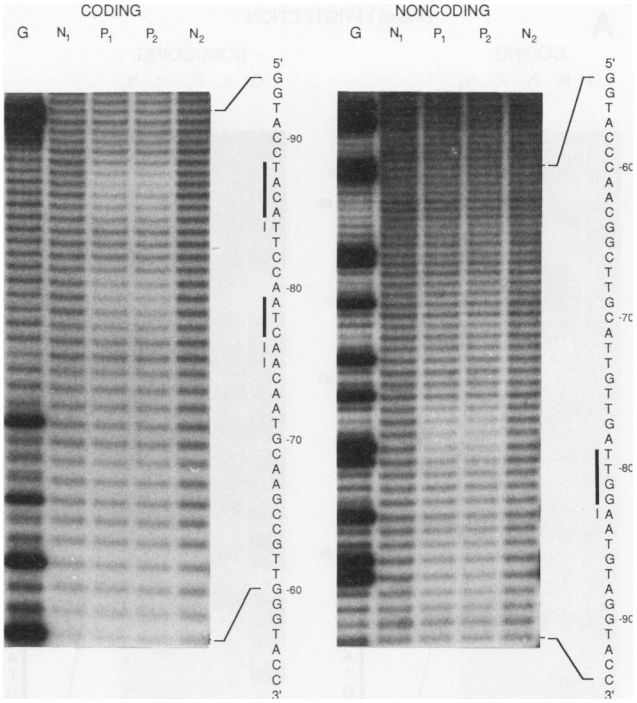

FIG. 3. Hydroxyl radical protection footprinting analysis with the nonfusion AbaA protein. N indicates reaction mixes containing no protein, and P indicates reaction mixes containing the native AbaA protein. The N_1 and P_1 reaction mixes contained 1 μg of poly(dI-dC) competitor, and the N_2 and P_2 reaction mixes contained 10 μg. Lanes marked G contained guanine-specific cleavage products of the probe. The regions that were strongly protected from hydroxyl radical cleavage are indicated by a thick bar, and those that were weakly protected are indicated by a thin bar. Coordinates relative to the transcription initiation site are shown.

by cloning the wild-type and mutant *A. nidulans* promoter fragments into the 2μm-based plasmid pYC7 (containing the *CYC1* minimal promoter fused to the *E. coli lacZ* gene) (15, 26).

Preparation and purification of the LacZ-AbaA fusion protein. The following procedure was used to minimize degradation of AbaA produced in *E. coli*. pUR291 and pAA37 were introduced into *E. coli* CSH26′ {*rpsL20* Δ(*pro-lac*) *recA56* [F′ *pro-lacZ*^{VU8}*I*^{q}]}. An overnight culture was diluted 100-fold in LB medium and grown at 30°C and 300 rpm to an A_{600} of 0.7 to 0.8 (4 to 5 h). Cells were induced with isopropyl-1-thio-β-D-galactopyranoside (IPTG; 1 mM) for 3 h at 30°C and 300 rpm, chilled to 0°C, pelleted at 4000 × *g* for 8 min at 4°C, washed with cold deionized water, resuspended in 3 volumes of lysis buffer (50 mM Tris-HCl [pH 8.0], 10 mM $MgCl_2$, 2 mM dithiothreitol [DTT], 20% glycerol), and frozen in liquid nitrogen. Cells were lysed by one passage through a French pressure cell at 16,000 lb/in^2, and lysates were cleared by centrifugation at 10,000 × *g* for 10 min. The supernatant was stored at −80°C. These crude extracts were estimated to contain approximately 0.1% LacZ-AbaA fusion protein.

The LacZ-AbaA fusion protein was purified by *p*-aminophenyl-β-D-thiogalactopyranoside-agarose affinity chromatography as described previously (54). Briefly, the cell lysate in lysis buffer was adjusted to 25 mM Tris-HCl (pH 8.0), 10 mM $MgCl_2$, 1.6 M NaCl, 10% glycerol, and 2 mM DTT and loaded onto the column. After extensive washing in the same buffer, the bound fusion protein was eluted with 3 column volumes of 0.1 M sodium borate (pH 10)–0.5 mM DTT, and the eluate was collected in an equal volume of 1 M Tris-HCl (pH 7.2). The eluate was concentrated and dialyzed against lysis or lysis-G (50 mM Tris-HCl [pH 8.0], 10 mM $MgCl_2$, 2 mM DTT) buffer and stored at −80°C.

Probe preparation and mobility shift assay. Plasmid-derived probes were labeled at one 3′ recessed end by using DNA polymerase I large fragment (Promega) or Sequenase (United States Biochemical), following the supplier's recommendations. The probes were purified by electrophoresis through a 6% polyacrylamide gel and recovered by electroelution at 300 V for 2 h in 0.2× TBE (Tris-borate-EDTA) buffer. For detection of promoter subfragments carrying AbaA binding sites, the promoters were isolated after gel electrophoresis, digested with restriction enzymes to yield two overlapping sets of fragments, end labeled with Sequenase, and precipitated twice with ammonium acetate and ethanol to remove free nucleotides.

Mobility shift assays were performed by using 1.0 to 1.8%

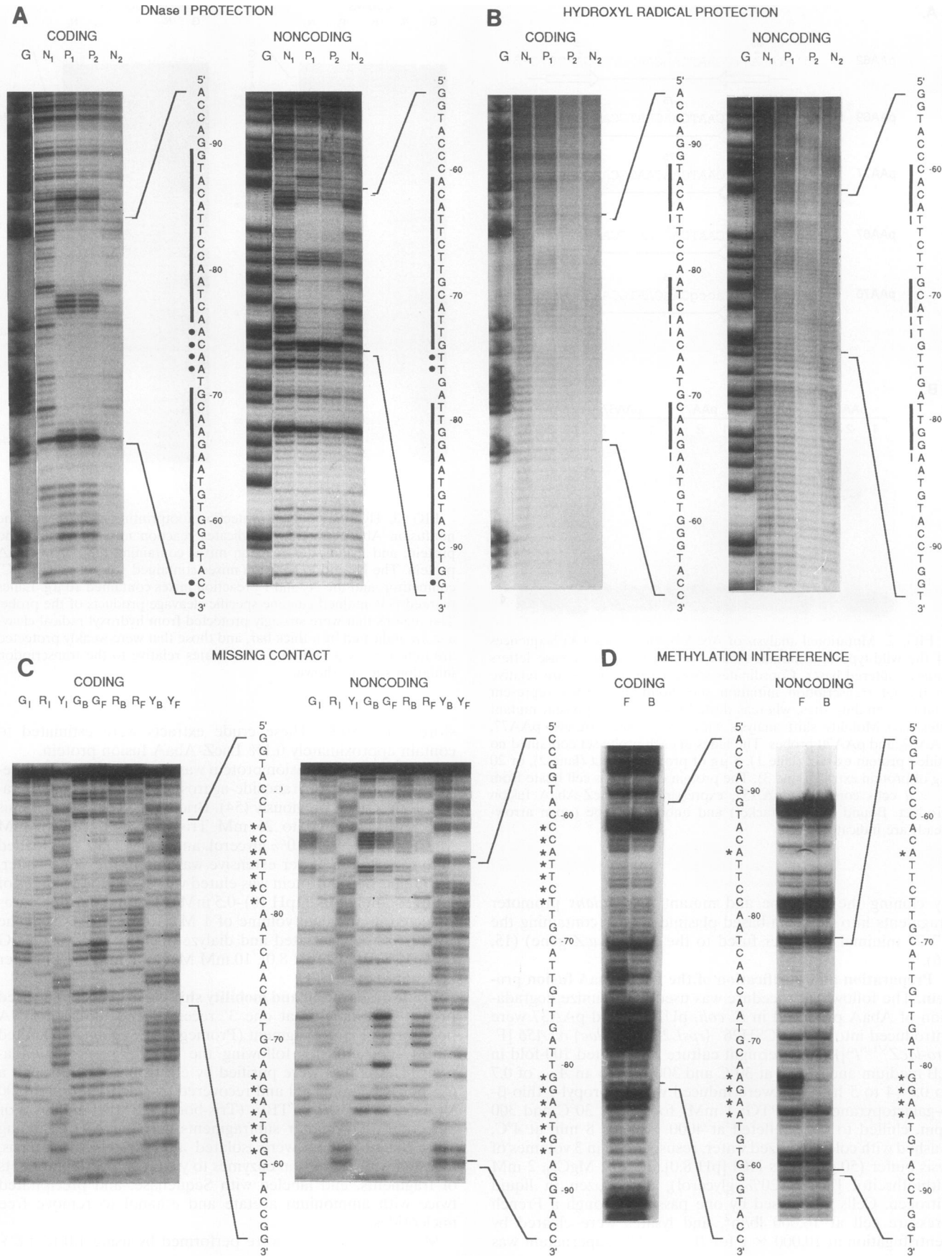
A
DNase I PROTECTION
CODING
NONCODING
G N1 P1 P2 N2
B
HYDROXYL RADICAL PROTECTION
CODING
NONCODING
G N1 P1 P2 N2
C
MISSING CONTACT
CODING
NONCODING
GI RI YI GB GF RB RF YB YF
D
METHYLATION INTERFERENCE
CODING
NONCODING
F B

agarose or 4 to 8% polyacrylamide (acrylamide-bisacrylamide, 79:1) gels with 0.5× TBE buffer. Binding reactions were set up in a 30-μl final volume with approximately 10 to 30 fmol (5×10^4 dpm) of probe and 5 to 20 μg of crude extract or 0.3 to 0.6 μg of purified protein in bind buffer (25 mM HEPES [*N*-2-hydroxyethylpiperazine-*N'*-2-ethanesulfonic acid]-KOH [pH 7.6], 40 mM KCl, 1 mM disodium EDTA, 10% glycerol) containing 250 μg of bovine serum albumin per ml, 2.5 mM disodium EDTA, and 50 to 100 μg of poly(dI-dC) per ml. Reaction mixes were incubated for 20 min at 25°C, loaded onto the gel, and run at 2 V/cm (agarose) or 4 mA constant current (polyacrylamide) for 8 to 12 h at 4°C. Agarose gels were dried down under vacuum onto nylon membrane supports. Polyacrylamide gels containing 2.5% glycerol were dried down under vacuum onto Whatman 3MM paper. Autoradiography was performed at room temperature with Kodak XAR film.

Specific competition mobility shifts were performed by setting up binding reaction mixes and incubating them for 15 min at 25°C. Specific competitor DNAs (pAA60 or pAA62) were added as intact subclones, as was nonspecific competitor DNA (pYC14) to yield equal amounts of DNA in each reaction mix and incubated for a further 15 min at 25°C prior to loading on a gel.

Protection footprinting assays. DNase I protection footprinting was performed as described previously (9) with the following modifications. The DNase I concentration was calibrated to yield 20 to 30% probe digestion in 2 min at 10°C in DFA buffer (10 mM Tris-HCl [pH 8.0], 5 mM $MgCl_2$, 1 mM $CaCl_2$, 2 mM DTT, 50 μg of bovine serum albumin per ml, 2 μg of calf thymus DNA per ml, 100 mM KCl). Binding reaction mixes (200 μl) containing 10^5 dpm of probe and 2 to 30 μg of purified protein were incubated at 10°C for 20 min, at which time DNase I was added. The reaction was allowed to proceed for 2 min at 10°C and inactivated by addition of stop buffer (0.3 M sodium acetate [pH 6.0], 10 μg of tRNA per ml, 20 mM disodium EDTA) and 1% sodium dodecyl sulfate (SDS) (final concentrations). Protein was removed by phenol-chloroform-isoamyl alcohol (50:50:1) extraction, and DNA was ethanol precipitated and resuspended in formamide sequencing-gel loading buffer. Products were fractionated in 6 or 10% denaturing polyacrylamide gels. The gels were fixed and dried, and autoradiography was performed at room temperature with Kodak XAR film.

Hydroxyl radical protection footprinting was performed essentially as previously described (53) under conditions established for the AbaA protein. Binding reaction mixes (85 μl) containing 10^5 dpm of probe were set up in bind-G buffer (25 mM HEPES-KOH [pH 7.6], 40 mM KCl, 1 mM disodium EDTA, 75 μg of bovine serum albumin per ml) with 2 μg of purified protein in lysis-G buffer and incubated at 10°C for 20 min. Hydroxyl radicals were generated by adding 5 μl of 2 mM $Fe(NH_4)(SO_4)_2$–4 mM disodium EDTA–0.06% H_2O_2–20 mM sodium ascorbate. The cleavage reaction mix (100 μl) was incubated for 2 min at 10°C, and the reaction was stopped with 10 μl of 0.1 M thiourea and 1 μl of 0.2 M disodium EDTA. Protein was removed by phenol-chloroform-isoamyl alcohol extraction, DNA was ethanol precipitated and resuspended in formamide gel-loading buffer. Products were fractionated in 6 or 10% denaturing polyacrylamide gels. The gels were fixed and dried, and autoradiography was performed at room temperature with Kodak XAR film.

Missing-contact footprinting. Missing-contact footprinting was performed as described previously (12). Briefly, end-labeled probes were chemically modified to remove either guanine, purine, or pyrimidine bases, and these probes were used in mobility shift assays with the purified LacZ-AbaA protein. The amount of protein added to each reaction mix was calibrated by mobility shift assay to yield an approximately 1 to 1 ratio of bound to free probe. Bound and free probes were localized by autoradiography of the intact gels, excised, and recovered by electroelution. After phenol-chloroform-isoamyl alcohol extraction and precipitation with ethanol, DNA was cleaved with 1 M piperidine at 90°C for 30 min (36). After three lyophilizations, the products were resuspended in formamide gel-loading dye and fractionated through 12% denaturing polyacrylamide gels. The gels were fixed, and autoradiography was performed directly at room temperature with Kodak XAR film.

Methylation interference footprinting. Probes for methylation interference footprinting were prepared as described previously (9). Modified probes were used in mobility shift assay reactions with purified LacZ-AbaA protein and processed as for missing-contact probes. The products were fractionated on 8% denaturing polyacrylamide gels.

***S. cerevisiae* transformation and β-galactosidase assays.** *S. cerevisiae* YPH500 [*ura3-52 lys2-801*^{amber} *ade2-101*^{ochre} *trp-Δ63 his3-Δ200 leu2-Δ1*] (45) was cultured and transformed as described previously (9, 25, 29). Cells were cotransformed with both expression and reporter plasmids and selected directly.

Assays for β-galactosidase activity were performed as described previously (9). Ten independent transformants were selected, pooled, and grown in appropriately supplemented medium containing glucose as a sole carbon source at 32°C and 300 rpm for 30 h. The cells were diluted 1:100 into appropriately supplemented medium containing either glucose or galactose as a sole carbon source and grown to an A_{600} of 0.3 to 0.4. Two independent experiments consisting of two replicate assays were performed in each case.

RESULTS

AbaA is a sequence-specific DNA-binding protein. Several lines of evidence suggested that AbaA was a sequence-specific DNA-binding protein (5, 8, 11, 13, 38). To test this hypothesis directly, we produced AbaA in *E. coli* as a β-galactosidase fusion protein (denoted LacZ-AbaA) and used it in mobility

FIG. 4. Protection, missing-contact, and interference footprint analysis with affinity-purified LacZ-AbaA protein and *yA*-derived probes. (A) DNase I protection analysis. N, P, and G are as defined in the legend to Fig. 3 except that the LacZ-AbaA fusion protein was used instead of the native AbaA protein. Protected regions are indicated by the solid bar along the sequence, and hypersensitive sites are marked with dots. Coordinates relative to the transcription initiation site are shown. (B) Hydroxyl radical protection analysis. Lanes are marked as in panel A. The regions that were strongly protected from hydroxyl radical cleavage are indicated by a thick bar, and those that were weakly protected are indicated by a thin bar. (C) Missing-contact interference analysis. G, R, and Y indicate probe modifications that specifically removed guanines, purines, or pyrimidines, respectively. Modified-input probe lanes are marked with the I subscript, fractionated bound-probe lanes are indicated with the B subscript, and free-probe lanes are denoted by the F subscript. Probe modifications that interfered with binding are indicated by asterisks next to the nucleotide sequence. Coordinates relative to the transcription initiation site are shown. (D) Methylation interference analysis. Lanes marked F and B contained free and bound methylated probe, respectively. Methylated nucleotides that inhibited binding are denoted by asterisks next to the nucleotide sequence. Coordinates relative to the transcription initiation site are shown.

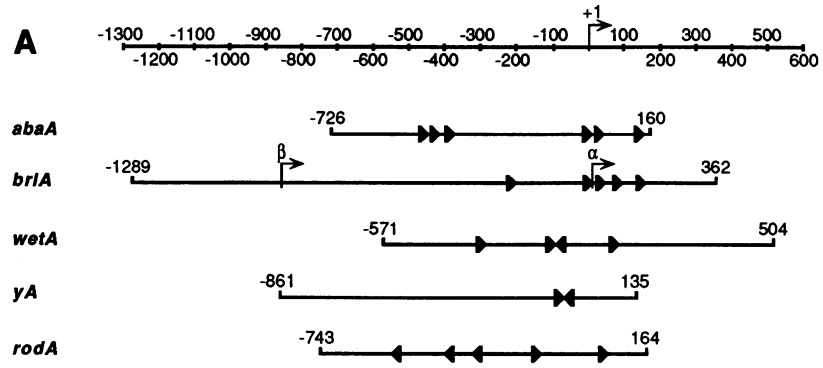

B

abaA	-502	TCCTAGGGCT TGACCTTTCA	CATTCC	AGTCGTACTA TTCGTAATAC	-457
	-470	ACTATTCGTA ATACCCTCAG	CATTCC	AAACATGACG ATGTACGAGT	-425
	-428	GAGTGGCCAT TGATACGCTG	CATTCC	TCTGAGCGAT CTTGCCACTG	-383
	-33	CACCATGCTG CTCGCTTCCA	CATTCT	CTTTCCCAGG CTCTTACATT	+13
	-11	TTCTCTTTCC CAGGCTCTTA	CATTCT	CTCTTCCAAG CATCTACGTT	+35
	+104	TCGTCTTTGG AATTTGTTCT	CATTCT	TGGGAGCGAA TCTTGGGGTC	+150
brlA	-234	TCTAGGAACT CGATAGCCTA	CATTCC	TGGCCTTGCT CGGGACCTGG	-189
	-32	TTCATCCGCC GCTCCTCCTC	CATTCC	GGCTCCCCAA CCTTCATTCT	14
	-12	CATTCCGGCT CCCCAACCTT	CATTCT	CTCTCTTCAC CAACTCGCTC	34
	57	CTTACACCCA CTCTGGTCTT	CATTCT	TTTGCTTTGC TCTTCTTCTG	102
	119	TGTCGAGATT AGCCCTCTTT	CATTCC	TTCACTGGCC TCCACTGGCC	164
wetA	-332	TCTGGCGTAG TGAAGCGTTG	CATTCC	GGCGGGTGGC CATTCAGCAT	-287
	-142	CCCGCCAGGT CGTTAGTCCG	CATTCC	TCTCCCACTA TAGAACGACT	-97
	-69	AGCCTCTGAA TTTCCCTTTG	CATTCC	AGTCGTTCTA TAGTGGGAGA	-114
	36	GGTTCCAACG CGCTGCGCTG	CATTCC	ATCTGCGCCC TCGACCATAC	81
yA	-106	GTCGCGTTCA GCACCAGGTA	CATTCC	AATCAACAAT GCAAGAATGT	-61
	-40	GATATATACT TCGCGTTTCA	CATTCT	TGCATTGTTG ATTGGAATGT	-85
rodA	-517	GTATGCAAGT AGTCAGTTCA	CATTCC	TCGGAGCTTT GCGACCAGCT	-562
	-370	TGCATCCCAG CATTTCTTGC	CATTCC	AAAATGTCAA ACTGTCAATC	-415
	-292	CTGCGTACTC AATACTGTCT	CATTCC	CCTGCTCCAG CTCTGTAGAT	-337
	-165	GCTCTGTTCC TTGCGTGGTG	CATTCC	AAAGACCCAT GAGGGAAGAA	-120
	5	TCATAGACAG TCCAGTCCCT	CATTCT	CAAGCCTCTT CTCCAAAAAC	50
CONSENSUS			**CATTCY**		

C

rodA	-541	GAATGTGAAC TGACTACTTG	CATACC	ACGAGATGAC TGCGGCTGAT	-496
	-98	AACCACGTCC TTGTTCAGAG	AATTCT	TCCCTCATGG GTCTTTGGAA	-143

FIG. 5. Identification of AbaA binding sites in developmentally regulated genes. (A) Mobility shift and DNase I protection assay probes. The scale at the top gives the transcription initiation sites (+1) and coordinates on either side. Below are the 5′ regions from several developmentally regulated genes, aligned at the transcription initiation site and marked with their terminal coordinates. Mobility shift and DNase I footprint assays were used to identify AbaA binding sites, and their locations and orientations are indicated by arrowheads. For *brlA*, both the *brlA*α and *brlA*β transcription initiation sites (42) are shown. (B) DNase I protection footprinting analysis. Nucleotide sequences spanning the AbaA DNA-binding

shift studies with probes from the *cis*-acting regulatory region of the *yA* conidial pigmentation gene (7). Attempts to produce significant quantities of the nonfusion protein were unsuccessful because of rapid proteolysis (6). Therefore, we used nonfusion AbaA only in selected experiments to compare its properties with those of the fusion protein. Figure 1A shows that *yA* 5′-flanking DNA contains inverted repeats, present in a region essential for developmental regulation of *yA* (8), similar to TEF-1 binding sites (20, 24, 56). Figure 1B shows that extracts containing the LacZ-AbaA protein bound to overlapping *yA* probes, whereas control extracts lacking the fusion protein did not. We investigated binding specificity by maintaining a constant ratio of probe to protein extract and adding various amounts of nonspecific competitor DNA. Figure 1C shows that even at a 1.2×10^4-fold mass excess of nonspecific competitor, no significant decrease in DNA binding occurred, demonstrating that the LacZ-AbaA product bound with high affinity.

We showed that this high binding affinity was sequence specific in competition experiments with DNA fragments from this region of *yA* (pAA60 and pAA62) as competitors against the pAA62 probe. Figure 1D shows that as the molar excess of pAA60 or pAA62 was increased, the amount of bound pAA62 probe was reduced. The slight difference in the ability of pAA60 and pAA62 to act as competitors suggests that the sequences immediately 5′ of one AbaA binding site, present in pAA60 but not in pAA62, stabilize DNA-protein binding. The results of missing-contact footprint analysis support this conclusion (see below). The presence of DNA similar in construction to pAA60 and pAA62 but containing an insert lacking putative AbaA binding sites in each reaction mix demonstrated that vector sequences play no part in the observed competition.

We tested the DNA sequence specificity of the LacZ-AbaA product with *yA* oligonucleotides containing four transversions within or overlapping one or both of the putative AbaA binding sites (Fig. 2A). Figure 2B shows the results of mobility shift analysis with wild-type and mutant probes. Mutations in both putative binding sites abolished DNA binding (probe pAA69), whereas mutations in either one of the sites alone severely inhibited DNA binding (probes pAA67 and pAA77). A mutation in the 3′ nucleotide of one site inhibited DNA binding slightly (probe pAA70). The two-site requirement for high-affinity binding was not evident for the nonfusion AbaA protein produced in *E. coli* (data not shown). Significant DNA binding was evident with oligonucleotides mutated at a single site (probes pAA67, pAA77, and pAA70), indicating that the observed requirement for two sites with the fusion protein was primarily, if not exclusively, due to the β-galactosidase moiety. However, as with the fusion protein, no DNA binding was evident with a probe containing mutations in both sites (pAA69). Therefore, AbaA binding is sequence specific and probably requires only a single site for a stable interaction.

The ability of the nonfusion AbaA protein to bind to a single site was examined by DNase I and hydroxyl radical protection footprinting with probes containing one (pAA77) or both (pAA62) sites. The affinity of the nonfusion protein for these two probes did not differ significantly (data not shown). In addition, DNase I and hydroxyl radical footprints were representative of those obtained with the fusion protein (see below). Figure 3 shows that AbaA produced three hydroxyl radical footprints of 5 bp over a single binding site. This footprinting pattern was identical to that obtained with the fusion protein (see Fig. 4B). Hence, the nonfusion and fusion AbaA proteins contact their binding sites in the same manner.

Contacts between AbaA and the AbaA binding sequence. We purified the AbaA fusion protein by affinity chromatography and used it for DNase I and hydroxyl radical protection, missing-contact, and methylation interference footprint analyses with the *yA*-derived pAA60 or pAA62 probe. Figure 4A shows that AbaA protected regions on each strand from DNase I cleavage. The protected regions extend from −89 to −76 and −70 to −57 on the coding strand and from −61 to −74 and −79 to −92 on the noncoding strand. The protected regions were centered over the predicted 5′-CATTCY-3′ binding sites. In addition, hypersensitive sites occurred on the 3′ side of each protected region. These maxima were especially prominent between the two binding sites, suggesting that significant DNA bending occurs in this region.

We used hydroxyl radical protection analysis (53) to identify the intimate interactions between AbaA and DNA. The results are shown in Fig. 4B. AbaA protected three regions of 5 bp on each strand. Regions of maximal protection encompassed positions −88 to −85, −79 to −77, and −69 to −66 on the coding strand and −60 to −63, −69 to −71, and −79 to −82 on the noncoding strand. The two outermost protected regions on each strand overlapped the predicted 5′-CATTCY-3′ binding sites.

We performed missing-contact footprint analysis (12) to determine which bases are required for AbaA binding. Figure 4C shows that removal of any of the bases in the sequence 5′-CATTCC-3′ (−86 to −81) or 5′-AGAATG-3′ (−67 to −62) on the coding strand had a marked effect on DNA binding, as revealed by the deficiency of these cleavage products in the bound probe fraction. The same pattern occurred for noncoding strand probes, identifying the sequences 5′-CATTCT-3′ (−62 to −67) and 5′-GGAATG-3′ (−81 to −86) as essential. These results established the essential DNA binding contacts as 5′-CATTCY-3′. Removal of the base immediately 5′ to this consensus site (the A at −87 and the G at −61 on the coding strand or the C at −61 and the T at −87 on the noncoding strand) had a less pronounced effect. This was consistent with the different effects of pAA60 and pAA62 in competition experiments (Fig. 2C).

The hydroxyl radical protection footprint results indicated that AbaA makes intimate backbone contacts across a major and a minor groove (see Discussion). We therefore performed methylation interference assays to assess the contribution of major- and minor-groove base-specific contacts on DNA binding. Figure 4D shows that methylated residues inhibiting AbaA binding occurred at positions −85 (A), −67 (A), −66 (G), −65 (A), and −64 (A) on the coding strand and −63 (A), −81 (G), −82 (G), −83 (A), and −84 (A) on the noncoding strand. Methylation interference at G residues indicated association of AbaA with the major groove, as guanine bases are methylated at the N7 position in the major groove. Methylation interference at A residues indicated that AbaA makes

sites are aligned. The terminal coordinates are indicated, and the nucleotides protected from DNase I cleavage are underlined. A consensus sequence for AbaA binding is presented at the bottom. Binding sites are boxed through all the sequences. (C) DNase I protection footprinting analysis of variant sites. Nucleotide sequences spanning the two variant AbaA DNA-binding sites in the *rodA* 5′-flanking region, identified by using high levels of AbaA, are aligned. The terminal coordinates are indicated, and the nucleotides protected from DNase I cleavage are underlined. Nucleotides that differ from the consensus AbaA binding site are marked by asterisks.

TABLE 1. AbaA-mediated β-galactosidase expression in *S. cerevisiae*[a]

Promoter (coordinates)	Expt	β-Galactosidase activity ($\Delta A_{420} \cdot min^{-1} \cdot ml^{-1} \cdot A_{600}^{-1}$)					
		Glucose			Galactose		
		−AbaA	+AbaA	Fold induction	−AbaA	+AbaA	Fold induction
abaA (−726 to −357)	1	0.43	0.45	1.05	0.24	0.17	0.71
	2	0.26	0.23	0.88	0.23	0.27	1.17
abaA (−349 to +159)	1	0.63	0.61	0.97	0.32	8.29	25.91
	2	0.40	0.46	1.15	0.34	6.10	17.94
abaA (−726 to +159)	1	0.33	0.26	0.79	0.06	2.11	35.17
	2	0.22	0.17	0.77	0.05	1.19	23.80
wetA (−156 to +333)	1	0.31	0.24	0.77	0.26	0.25	0.96
	2	0.26	0.19	0.73	0.34	0.36	1.06
wetA (−571 to −7)	1	0.11	0.06	0.55	0.11	2.58	23.45
	2	0.06	0.06	1.00	0.06	1.16	19.33
wetA (−571 to +318)	1	0.83	1.11	1.34	0.69	0.74	1.07
	2	0.52	0.83	1.60	0.53	0.65	1.23
brlA (−308 to +257)	1	19.60	15.18	0.77	50.08	195.81	3.91
	2	19.03	16.29	0.86	37.56	153.37	4.08
rodA (−598 to −299)	1	0.03	0.05	1.67	0.11	0.78	7.09
	2	0.11	0.11	1.00	0.04	0.45	11.25
rodA (−299 to +235)	1	1.63	1.86	1.14	1.44	4.09	2.84
	2	1.56	2.11	1.35	1.89	2.98	1.58
rodA (−748 to +235)	1	0.15	0.15	1.00	0.39	0.65	1.67
	2	0.60	0.25	0.42	0.21	0.49	2.33
None	1	0.15	0.05	0.33	0.20	0.27	1.35
	2	0.11	0.09	0.82	0.06	0.12	2.00

[a] The results of two independent experiments are shown. Each value represents the average of two assays. Variability between assays was less than 10%.

essential minor-groove contacts, as adenine bases are methylated at the N3 position in the minor groove.

AbaA binding sites are present in developmentally regulated genes. We examined the 5′-flanking regions of several developmentally regulated genes thought to be direct or indirect targets for *abaA*. These were the upstream regulatory gene *brlA* (1, 42), the downstream regulatory gene *wetA* (35), and the *rodA* structural gene, encoding the conidial rodlet layer protein (51). The 5′-flanking regions of these genes contain multiple copies of the AbaA binding site sequence 5′-CAT TCY-3′. Interestingly, the 5′-flanking region of *abaA* also contains a number of such sites (38). Figure 5A shows the 5′ regions of the genes used for mobility shift assay identification of functional binding sites and the location and orientation of 5′-CATTCY-3′ sequences. DNase I footprint analysis with partially purified AbaA fusion protein showed that all of the predicted binding sites were protected (data not shown). The protected sequences are underlined in Fig. 5B. Alignment of the protected sequences confirmed the AbaA binding sequence as 5′-CATTCY-3′. Figure 5C shows two AbaA binding sites in the *rodA* 5′ region that differed from the consensus by one nucleotide and were only protected by large amounts (30 μg) of LacZ-AbaA (data not shown). Therefore, AbaA can interact with and may be directly involved in the regulation of the upstream regulatory gene *brlA*α, the downstream regulatory gene *wetA*, *abaA* itself, and the structural genes *rodA* and *yA*.

AbaA is a transcriptional activator. The results from studies of loss- and gain-of-function *abaA* mutations were consistent with the hypothesis that AbaA is a transcriptional activator in *A. nidulans* (11, 38). AbaA activator function was also demonstrated for the *yA* gene in an *S. cerevisiae* heterologous gene expression system, in which functional AbaA and intact binding sites were essential for transcriptional activation (8). We

TABLE 2. β-Galactosidase expression from mutant *yA* sequences[a]

Construct	Expt	β-Galactosidase activity ($\Delta A_{420} \cdot min^{-1} \cdot ml^{-1} \cdot A_{600}^{-1}$)					
		Glucose			Galactose		
		−AbaA	+AbaA	Fold induction	−AbaA	+AbaA	Fold induction
pAA62 (wild type)	1	0.08	0.03	0.37	0.16	6.29	39.31
	2	0.11	0.11	1.00	0.11	4.66	42.36
pAA69 (double mutant)	1	0.29	0.03	0.10	0.18	0.21	1.17
	2	0.15	0.11	0.73	0.07	0.11	1.57
pAA77 (single mutant)	1	0.02	0.03	1.50	0.16	0.20	1.25
	2	0.10	0.10	1.00	0.07	0.09	1.29
pAA67 (single mutant)	1	0.11	0.07	0.64	0.18	0.19	1.06
	2	0.11	0.13	1.18	0.07	0.21	3.00
pAA70 (single mutant)	1	0.06	0.07	1.17	0.06	0.08	1.33
	2	0.06	0.05	0.83	0.05	0.07	1.40

[a] The results of two independent experiments are shown. Each value represents the average of two assays. Variability between assays was less than 10%.

TABLE 3. Binding sites of proteins containing the ATTS DNA-binding motif

Factor (reference)	Binding site	Sequence[a] (references)
AbaA (this study)	Consensus	CATTCY
	rodA variant 1	CATACC
	rodA variant 2	AATTCT
	yA mutant	CATTCA
TEF-1 (20)	GT-IIC	CACATTCCA
	Sph-I	TGCATGCTT
	Sph-II	TGCATACTT
	GT-IIA	GACTTTCCA
	Polyomavirus wild type	AACATTCTA
	Polyomavirus EC9.1	TTCATCCA
MCBF (34)	M-CAT 1 (cTNT)	CATTCCT
	M-CAT 2 (cTNT)	CATTCCT
	M-CAT (α-actin)	CATTCCT
TEC1p (31)	Ty1 enhancer B1	CTTTCC (19, 22)
	Ty1 enhancer B2	CTTTCC (19, 22)

[a] Matches to the AbaA consensus binding site are underlined.

exploited an *S. cerevisiae* heterologous gene expression system (15) to test the hypothesis that AbaA directly activates transcription by binding to 5'-flanking sequences of potential target genes. We fused an intronless version of *abaA* to the *S. cerevisiae GAL1* promoter on the centromeric plasmid pAA54. We then inserted the *A. nidulans* 5'-flanking regions containing AbaA binding sites upstream of a minimal *CYC1* promoter fused to the *E. coli lacZ* gene in pYC7 (15, 26). We transformed these plasmids into *S. cerevisiae* and grew the resultant strains under noninducing (glucose) or inducing (galactose) conditions. Table 1 shows that production of β-galactosidase was induced by *abaA* expression for at least one promoter fragment construct for each of the genes. In the case of the *brlA*α-containing construct, significant expression also occurred under noninducing and inducing conditions in the absence of *abaA*. These results support the proposal that AbaA is a transcriptional activator functioning through the AbaA binding sites in the *cis*-acting regulatory regions of target genes.

Mutations in both of the binding sites in the *yA* promoter abolished AbaA-mediated transcriptional activation in the *S. cerevisiae* heterologous gene expression system (Table 2). We tested the *yA* promoter-derived mutants shown in Fig. 2, containing mutations in one of the two binding sites, in the same system. Table 2 shows that single AbaA binding sites are insufficient for activation, even though the nonfusion AbaA protein binds stably to a single site in vitro.

DISCUSSION

The *A. nidulans abaA* gene controls the expression of numerous morphogenetic and several other developmental regulatory loci (38). The data presented in this article show that *abaA* encodes a DNA-binding protein (AbaA) that specifically recognizes the sequence 5'-CATTCY-3'. This sequence is encompassed by the previously identified binding sites for another protein containing the ATTS DNA-binding motif, TEF-1, which binds to the GT-IIC enhanson of simian virus 40 and to the polyomavirus enhancer (20). This sequence is also encompassed by the binding site for the M-CAT binding factor (MCBF), which binds to the M-CAT 1 and 2 activating sequences of chicken skeletal troponin and an unnamed site of chicken α-actin (34). MCBF is closely related, and possibly identical, to TEF-1 (23). The ATTS binding site is also included in the previously described Inr sequence (5'-CCT CATTCTGG-3') (47) and is present in several *A. nidulans* developmentally regulated genes, including *brlA* (1), *abaA* (2, 38), and *trpC* (27). Thus, AbaA and these other factors may bind to DNA and interact with the transcription initiation complex at the point of transcription initiation as well as at sites upstream and downstream of initiation (Fig. 5; Table 3 and references therein). This could explain why constructs containing only short regions around the transcription initiation sites of *trpC* (27) and *abaA* (2) retained developmental regulation.

Unlike many other eukaryotic DNA-binding motifs, the ATTS motif has a highly conserved binding specificity. Our results show that all CATTCY sequences in the 5'-flanking regions of the developmentally regulated genes examined are bound by AbaA. Sequences differing from the consensus binding site by a single base in the first or fourth position were present in the 5' region of *rodA* but produced DNase I footprints only in the presence of high levels of AbaA (Fig. 5C). TEF-1 also binds to the Sph-I and -II enhansons, containing sites that differ from CATTCY by one nucleotide in the fourth position (Table 3), with 10-fold and 3- to 4-fold lower affinity, respectively, relative to the GT-IIC enhanson (20). The AbaA and TEF-1 biochemical data are consistent with in vivo transcription activation results from systematically mutated M-CAT binding sites (23). The *S. cerevisiae* Ty1 enhancer, which may interact with TEC1p, another protein containing the ATTS motif (31), contains potential recognition sequences which differ by one nucleotide in the second position (Table 3). Therefore, the ATTS DNA-binding motif has high selectivity for the sequence CATTCY but can tolerate slight variations, with a concomitant reduction in binding affinity.

The results from our in vitro DNA-binding studies show that AbaA binds to a single site with high affinity. In addition, the orientation and spacing of two sites had little effect on binding (data not shown). These data suggest that, unlike TEF-1, AbaA binding to two sites may not be cooperative. Conversely, in vivo transcriptional activation by AbaA appears to be sensitive to orientation and spacing of sites. Although it binds to a single site, no transcriptional activation was detected in the *S. cerevisiae* heterologous expression system (Table 2). Similarly, a number of promoter fragments containing AbaA binding sites from developmentally regulated genes failed to respond to AbaA-mediated transcriptional activation in this heterologous system (Table 1). In these cases, other *A. nidulans* factors may be required for AbaA activity from these sites, AbaA may function negatively to repress expression from particular combinations of sites, or *S. cerevisiae* factors may be interfering with AbaA function. The properties of MCBF are similar to those of AbaA in that a single site is a good binding substrate and spacing does not have a significant effect on DNA binding, although in vivo activity is altered (34). AbaA contains a potential leucine zipper lacking an associated basic region (38) but does not appear to function as a dimer. This is supported by results from deletion analysis showing that the region containing the potential leucine zipper is not required for AbaA activity in *A. nidulans* (6). Therefore, AbaA binds to a single site with high affinity in vitro but requires two or more sites to activate transcription in vivo.

Protein structure predictions of AbaA suggested that the ATTS motif consists of an α-helix and two β-sheets, which may constitute a β-ribbon (5). β-sheets and β-ribbons are important determinants of minor-groove binding for several DNA-binding proteins, including HU, IHF, TFIID, and MetJ (32, 39, 48, 49, 55, 57). The predicted α-helix and β-sheet structure of the ATTS DNA-binding motif may be analogous to that of the C_2H_2 Zn^{2+} DNA-binding motif, consisting of an α-helix

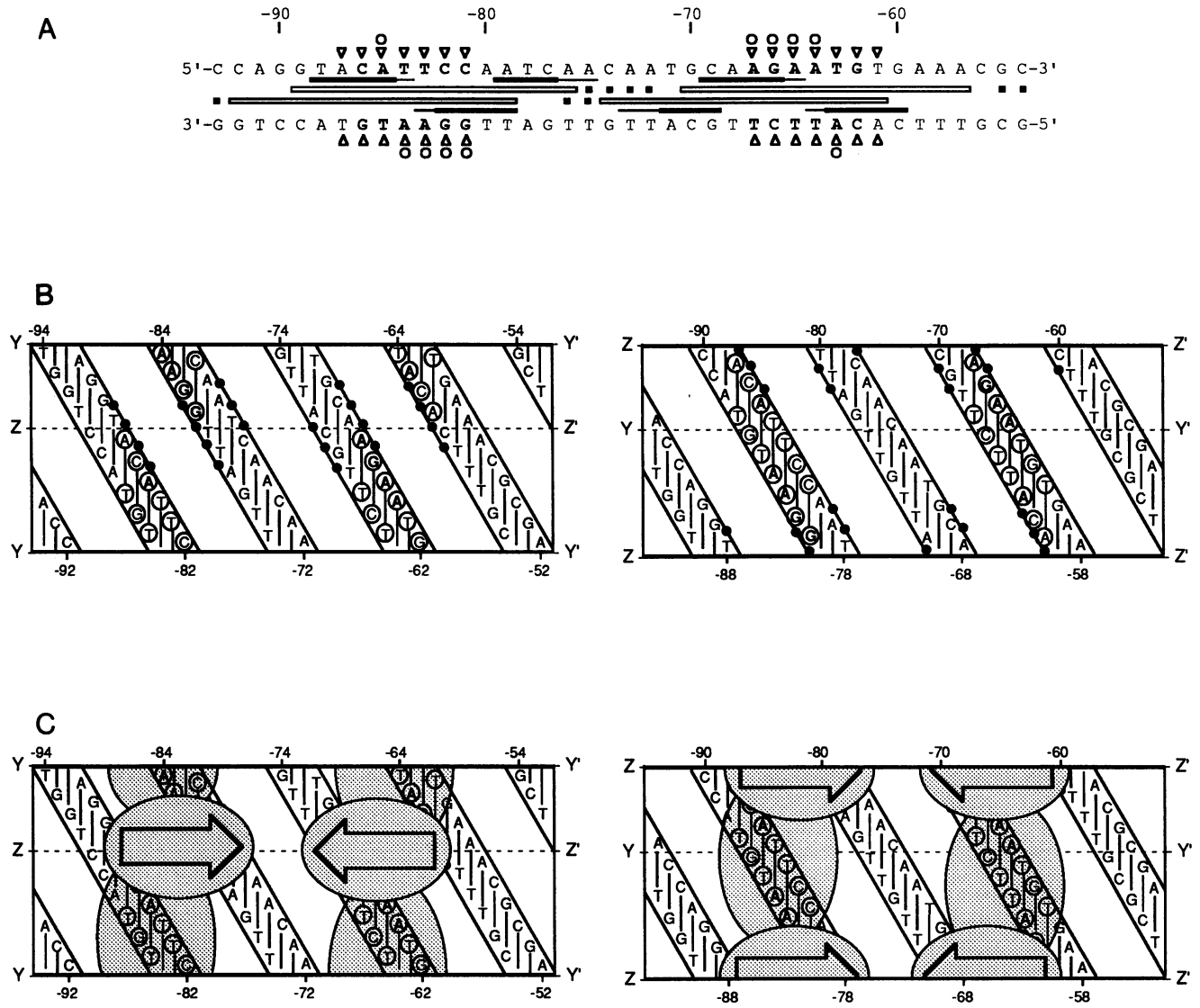

FIG. 6. Proposed structure of the AbaA-DNA complex. (A) Summary of results from footprint analyses. A partial nucleotide sequence of the *yA* 5′-flanking region is shown, with the AbaA binding sites shown in boldface type. Coordinates above the sequence are relative to the *yA* transcription initiation site. Open circles identify nucleotides required for AbaA binding in the methylation interference assay. Open triangles identify nucleotides required for AbaA binding in the missing-contact footprinting assay. Nucleotides that are highly protected from hydroxyl radical cleavage by bound AbaA are indicated by a solid bar, and those that are weakly protected are indicated by a thin line. Nucleotides protected by bound AbaA from DNase I cleavage are indicated by an open bar, and hypersensitive sites are marked with solid squares. (B) Two-dimensional cylindrical projection of a DNA double helix. The base pairs are drawn across the minor groove, with the sequence of the *yA* 5′-flanking region shown. Coordinates relative to the *yA* transcription initiation site are shown at the top for the noncoding strand and at the bottom for the coding strand. Nucleotides highly protected from hydroxyl radical cleavage are marked by a solid circle on the DNA backbone directly above (coding strand) or below (noncoding strand) the base. Circles identify bases that were required for AbaA binding in the missing-contact assay. Bases shown in boldface type were required for AbaA binding in the methylation interference assay. The two cylindrical projections show the DNA double helix from opposite sides, so that the dotted line through the left projection (Z-----Z′) represents the boundaries of the right projection and the dotted line through the right projection (Y-----Y′) represents the boundaries of the left projection. (C) AbaA-DNA complex. AbaA protein is represented as two shaded ellipses, one pair over each binding site. The opaque ellipses show DNA backbone contacts, and the translucent ellipses show base-specific contacts in the major and minor grooves. The arrows designate the relative orientations of the protein molecules.

tethered to a β-ribbon by the coordination of a Zn^{2+} ion (10). In view of these potential structural parallels and the lack of detailed information about interactions between DNA and ATTS DNA-binding proteins, we performed an analysis designed to gain a better understanding of the interactions between AbaA and its binding sites.

Figure 6 presents a model for the AbaA-DNA interaction based on the data presented in this article. Hydroxyl radical protection footprint analysis showed that only one face of the helix is in intimate contact with AbaA, as the three footprint minima on the coding strand were spaced approximately one helical turn apart, as were those on the noncoding strand (Fig. 4B and 6A). Intimate contact occurs between AbaA and DNA across a major and a minor groove, as evidenced by the

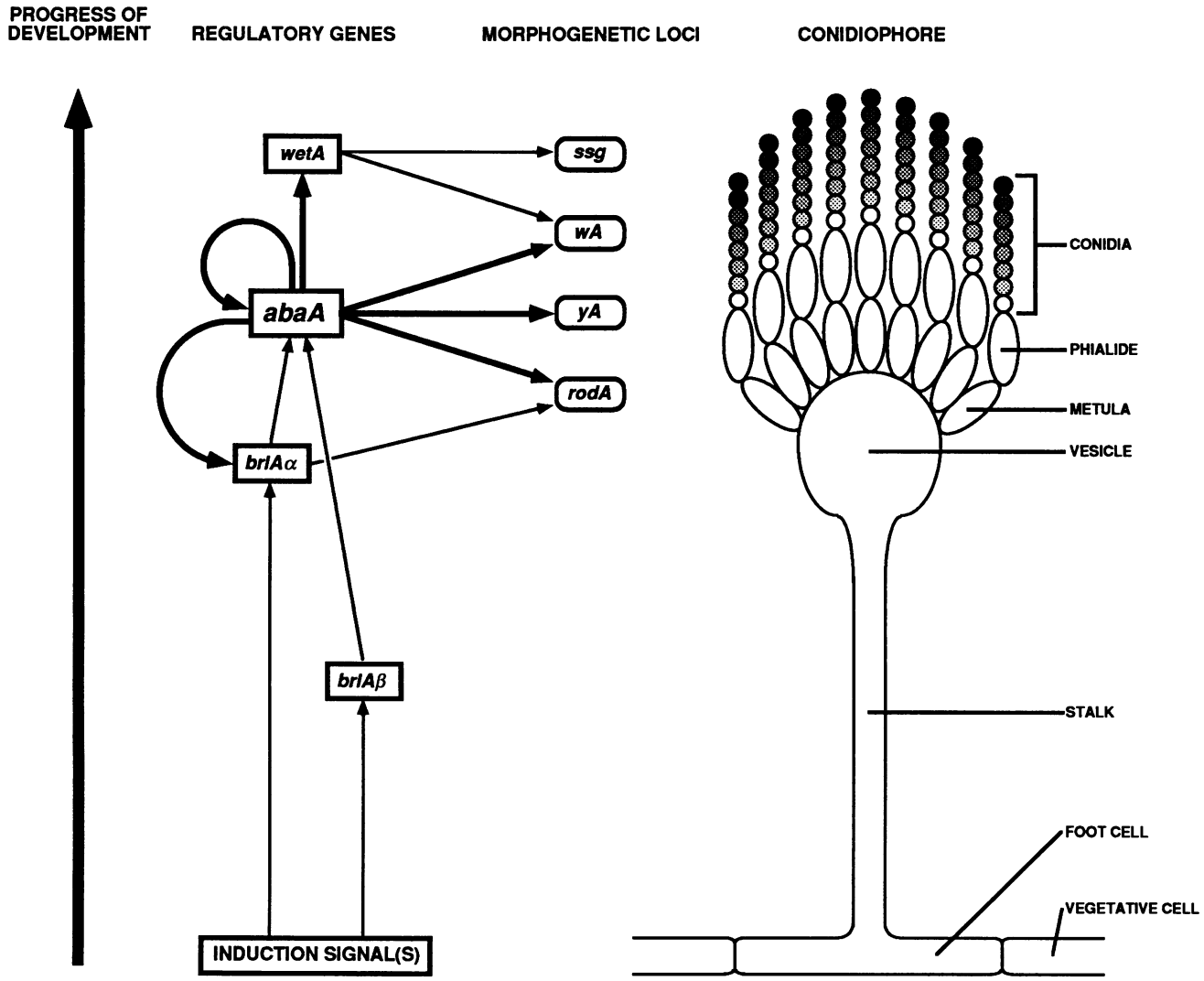

FIG. 7. Model for feedback controls established by AbaA. The central regulatory pathway controlling development in *A. nidulans* is aligned with a diagrammatic representation of a conidiophore to relate time of gene expression with development. The cell types of the conidiophore are indicated. Direct regulatory interactions demonstrated genetically and biochemically (thick arrows) and regulatory interactions proposed on the basis of genetic analysis (thin arrows) are shown. An induction signal(s) initiates the pathway leading to the activation of *brlA*α and *brlA*β. *brlA*α- and/or *brlA*β-mediated events activate *abaA*. AbaA activates *brlA*α, reinforces its own transcription, and activates *wetA*. The regulatory loops established by *abaA* lead to phialide differentiation and developmental determination. These regulatory products activate the expression of numerous structural genes whose products contribute to the form and function of the conidiophore (e.g., *rodA*, *yA*, and *wA*). *wetA* activates numerous spore-specific genes (*ssg*) required for spore maturation.

positions of the three minima over a single binding site (Fig. 4B and 6A). For the distal AbaA binding site in the *yA* promoter, the protected region on the noncoding strand (−80 to −82) is displaced by 6 bp in the 3′ direction relative to the protected region on the coding strand (−88 to −85). Similarly, the second protected region on the coding strand (−79 to −77) is displaced by 3 bp in the 3′ direction relative to the protected region on the noncoding strand (−80 to −82). The same pattern is evident for the proximal AbaA binding site in the *yA* promoter, but in this instance, the order is inverted, as is the orientation of the site. The closest points across a major groove are displaced by 7 bp, and those across a minor groove are displaced by 3 bp. Therefore, the hydroxyl radical footprints show that AbaA spans the major and minor grooves. The two sets of three adjacent minima encompassing each binding site exhibit dyad symmetry around the central G-C base pair at position −74 of the *yA* promoter (Fig. 4B and 6A), further supporting the proposal that each AbaA protein molecule contacts one binding site. The results from methylation interference experiments (Fig. 4D and 6A) showed that methylation of residues in either the major or minor groove inhibited AbaA binding, supporting the conclusion that the protein makes essential contacts in both grooves. Only a few other proteins make essential contacts in both grooves (4, 40, 46). Furthermore, this observation is consistent with the proposed interactions between β-sheets and the minor groove of DNA (16). Contacts across a major and minor groove occur commonly with protein dimers over a binding site with dyad symmetry (21, 53), but in the case of AbaA, symmetry within a single site is absent, and each monomer probably spans both

grooves. These results clearly demonstrate the unique DNA-binding properties of the ATTS DNA-binding motif.

Activation of numerous morphogenetic loci during conidiophore development in *A. nidulans* is largely controlled by the sequentially expressed activities of three regulatory genes, *brlA*, *abaA*, and *wetA* (52). Genetic evidence indicated that *brlA* was the first gene expressed, followed by *abaA* and finally *wetA*, constituting a linear regulatory pathway. Similar regulatory hierarchies have been proposed for other developmental systems, such as *Drosophila* embryogenesis and mammalian myogenesis (41, 50), and the complex molecular interactions are currently being elucidated. The data in this article present the molecular basis for one such developmental switch. They indicate that *abaA* is a direct regulator of *brlA* (*brlA*α) and *wetA* transcription, because AbaA binding sites are present in the *cis*-acting regulatory regions of both genes (Fig. 5) and these regions were capable of mediating transcriptional activation by AbaA in *S. cerevisiae* (Table 1) and *A. nidulans* (3). Our data further indicate that AbaA directly activates the *rodA* and *yA* structural genes as well as the *wA* structural gene (37), whose products contribute directly to the form and function of the conidiophore. Thus, *abaA* regulates the transcription of structural and regulatory genes with critical developmental functions.

We have also shown that AbaA binds to its own *cis*-acting regulatory sequences and that these sequences mediate AbaA-directed transcriptional activation in *S. cerevisiae*. Thus, *abaA* is probably subject to positive autoregulation. The series of feedback loops established by *abaA*, shown in Fig. 7, imply that the developmental regulatory pathway is self-reinforcing; that is, once it is initiated by expression of *brlA*, its continued activity should become independent of the initiating signals. This could represent the molecular basis of the genetic switch that establishes developmental determination in this system, and other lines of evidence support this view. Ultrastructural studies showed that loss-of-function mutations in *abaA* block phialide development and lead to reiteration of the metula cell type (44). Mutant conidiophores can be transplaced into liquid medium, which suppresses sporulation, where the metulae dedifferentiate and grow as vegetative hyphae. This is also true of the conidiophore stalk cells produced in *brlA* mutants (3). Thus, conidiophore cell types produced prior to *abaA* activation are capable of returning to vegetative functions when placed in growth medium. By contrast, sporogenous phialide cells, produced upon activation of *abaA*, and other mature conidiophore cell types produced in the presence of the wild-type *abaA* product are apparently incapable of re-establishing vegetative growth. Moreover, phialide cell type determination by *abaA* requires the continued presence of its product. When temperature-sensitive *abaA* mutants are grown and allowed to sporulate at the permissive temperature and then shifted to the restrictive temperature, conidium production ceases and supernumerary metulae are produced by branching from existing metulae (44), consistent with interruption of a self-perpetuating regulatory pathway. A reciprocal temperature shift results in differentiation of distal metulae into phialides that go on to produce conidia, consistent with re-establishment of the regulatory pathway. In view of the results presented in this article, we propose that *abaA* acts as a genetic switch that, when turned on, establishes feedback loops resulting in developmental determination. It will be of interest to ascertain the effects on development of systematic elimination of individual feedback loops.

ACKNOWLEDGMENTS

We thank Lois Miller for critically reviewing the manuscript, our colleagues in the laboratory for their many helpful comments and suggestions, and Janis Antwine for expert secretarial assistance.

This work was supported by NIH grant GM-37886 to W.E.T. A.A. was partially supported by a grant from Myco Pharmaceuticals, Inc.

REFERENCES

1. **Adams, T. H., M. T. Boylan, and W. E. Timberlake.** 1988. *brlA* is necessary and sufficient to direct conidiophore development in *Aspergillus nidulans*. Cell **54**:353–362.
2. **Adams, T. H., and W. E. Timberlake.** 1990. Upstream elements repress premature expression of an *Aspergillus* developmental regulatory gene. Mol. Cell. Biol. **10**:4912–4919.
3. **Aguirre, J., M. A. Frizzell, and W. E. Timberlake.** Unpublished data.
3. **Anderson, J. E., M. Ptashne, and S. C. Harrison.** 1987. Structure of the repressor-operator complex of bacteriophage 434. Nature (London) **326**:846–852.
5. **Andrianopoulos, A., and W. E. Timberlake.** 1991. ATTS, a new and conserved DNA binding domain. Plant Cell **3**:747–748.
6. **Andrianopoulos, A., and W. E. Timberlake.** Unpublished data.
7. **Aramayo, R., and W. E. Timberlake.** 1990. Sequence and molecular structure of the *Aspergillus nidulans yA* (laccase I) gene. Nucleic Acids Res. **18**:3415.
8. **Aramayo, R., and W. E. Timberlake.** 1993. The *Aspergillus yA* gene is directly regulated by the *abaA* gene. EMBO J. **12**:2039–2048.
9. **Ausubel, F. M., R. Brent, R. E. Kingston, D. D. Moore, J. A. Smith, J. G. Seidman, and K. Struhl.** 1987. Current protocols in molecular biology. John Wiley & Sons, New York.
10. **Berg, J. M.** 1988. Proposed structure for the zinc-binding domain from transcription factor IIIA and related proteins. Proc. Natl. Acad. Sci. USA **85**:99–102.
11. **Boylan, M. T., P. M. Mirabito, C. E. Willet, C. R. Zimmerman, and W. E. Timberlake.** 1987. Isolation and physical characterization of three essential conidiation genes from *Aspergillus nidulans*. Mol. Cell. Biol. **7**:3113–3118.
12. **Brunelle, A., and R. F. Schleif.** 1987. Missing contact probing of DNA-protein interactions. Proc. Natl. Acad. Sci. USA **84**:6673–6676.
13. **Bürglin, T. R.** 1991. The TEA domain: a novel, highly conserved DNA-binding motif. Cell **66**:11–12.
14. **Campbell, S., M. Inamdar, V. Rodrigues, V. Raghavan, M. Palazzolo, and A. Chovnick.** 1992. The *scalloped* gene encodes a novel, evolutionarily conserved transcription factor required for sensory organ differentiation in *Drosophila*. Genes Dev. **6**:367–379.
15. **Chang, Y. C., and W. E. Timberlake.** 1993. Identification of *Aspergillus brlA* response elements (BREs) by genetic selection in yeast. Genetics **133**:29–38.
16. **Church, G. M., J. L. Sussman, and S.-H. Kim.** 1977. Secondary structural complementarity between DNA and proteins. Proc. Natl. Acad. Sci. USA **74**:1458–1462.
17. **Clutterbuck, A. J.** 1969. A mutational analysis of conidial development in *Aspergillus nidulans*. Genetics **63**:317–327.
18. **Clutterbuck, A. J., and W. E. Timberlake.** 1992. Genetic regulation of sporulation in the fungus *Aspergillus nidulans*, p. 103–120. *In* V. E. A. Russo, S. Brody, D. Cove, and S. Ottolenghi (ed.), Development: the molecular genetic approach. Springer-Verlag, New York.
19. **Company, M., and B. Errede.** 1988. A Ty1 cell-type-specific regulatory sequence is a recognition element for a constitutive binding factor. Mol. Cell. Biol. **8**:5299–5309.
20. **Davidson, I., J. H. Xiao, R. Rosales, A. Straub, and P. Chambon.** 1988. The HeLa cell protein TEF-1 binds specifically and cooperatively to two SV40 enhancer motifs of unrelated sequence. Cell **54**:931–942.
21. **Dixon, W. J., J. J. Hayes, J. R. Levin, M. F. Weidner, B. A. Dombroski, and T. D. Tullius.** 1992. Hydroxyl radical footprinting. Methods Enzymol. **208**:380–413.
22. **Errede, B., M. Company, and C. A. Hutchison.** 1987. Ty1 sequence with enhancer and mating-type-dependent regulatory activities. Mol. Cell. Biol. **7**:258–265.
23. **Farrance, I. K. G., J. H. Mar, and C. P. Ordahl.** 1992. M-CAT

binding factor is related to the SV40 enhancer binding factor, TEF-1. J. Biol. Chem. **267**:17234–17240.
24. **Fromental, C., M. Kanno, H. Nomiyama, and P. Chambon.** 1988. Cooperativity and hierarchical levels of functional organization in the SV40 enhancer. Cell **54**:943–953.
25. **Gietz, D., A. St. Jean, R. A. Woods, and R. H. Schiestl.** 1992. Improved method of high efficiency transformation of intact yeast cells. Nucleic Acids Res. **20**:1425.
26. **Guarente, L., and T. Mason.** 1983. Heme regulates transcription of the *CYC1* gene of *Saccharomyces cerevisiae* via an upstream activation site. Cell **32**:1279–1286.
27. **Hamer, J. E., and W. E. Timberlake.** 1987. Functional organization of the *Aspergillus nidulans trpC* promoter. Mol. Cell. Biol. **7**:2352–2359.
28. **Han, S., J. Navarro, R. A. Greve, and T. H. Adams.** 1993. Translational repression of *brlA* expression prevents premature development in *Aspergillus*. EMBO J. **12**:2449–2457.
29. **Ito, H., Y. Fukuda, K. Murata, and A. Kimura.** 1983. Transformation of intact yeast cells treated with alkali cations. J. Bacteriol. **153**:163–168.
30. **Kunkel, T. A.** 1985. Rapid and efficient site-specific mutagenesis without phenotypic selection. Proc. Natl. Acad. Sci. USA **82**:488–492.
31. **Laloux, I., E. Dubois, M. Dewerchin, and E. Jacobs.** 1990. *TEC1*, a gene involved in the activation of Ty1 and Ty1-mediated gene expression in *Saccharomyces cerevisiae*: cloning and molecular analysis. Mol. Cell. Biol. **10**:3541–3550.
32. **Lee, D. K., M. Horikoshi, and R. G. Roeder.** 1991. Interaction of TFIID in the minor groove of the TATA element. Cell **67**:1241–1250.
33. **Mar, J. H., and C. P. Ordahl.** 1988. A conserved CATTCCT motif is required for skeletal muscle-specific activity of the cardiac troponin T gene promoter. Proc. Natl. Acad. Sci. USA **85**:6404–6408.
34. **Mar, J. H., and C. P. Ordahl.** 1990. M-CAT binding factor, a novel *trans*-acting factor governing muscle-specific transcription. Mol. Cell. Biol. **10**:4271–4283.
35. **Marshall, M. A., and W. E. Timberlake.** 1991. *Aspergillus nidulans wetA* activates spore-specific gene expression. Mol. Cell. Biol. **11**:55–62.
36. **Maxam, A., and W. Gilbert.** 1980. Sequencing end-labeled DNA with base-specific chemical cleavages. Methods Enzymol. **65**:497–559.
37. **Mayorga, M. E., and W. E. Timberlake.** Unpublished data.
38. **Mirabito, P. M., T. H. Adams, and W. E. Timberlake.** 1989. Interactions of three sequentially expressed genes control temporal and spatial specificity in *Aspergillus* development. Cell **57**:859–868.
39. **Nikolov, D. B., S.-H. Hu, J. Lin, A. Gasch, A. Hoffman, M. Horikoshi, N.-H. Chua, R. G. Roeder, and S. K. Burley.** 1992. Crystal structure of TFIID TATA-box binding protein. Nature (London) **360**:40–46.
40. **Otting, G., Y. Q. Qian, M. Billeter, M. Muller, M. Affolter, W. J. Gerhing, and K. Wuthrich.** 1990. Protein-DNA contacts in the structure of a homeodomain-DNA complex determined by nuclear magnetic resonance spectroscopy in solution. EMBO J. **10**:3085–3092.
41. **Pinney, D. F., and C. P. Emerson.** 1992. Skeletal muscle differentiation, p. 459–478. *In* V. E. A. Russo, S. Brody, D. Cove, and S. Ottolenghi (ed.), Development: the molecular genetic approach. Springer-Verlag, New York.
42. **Prade, R. A., and W. E. Timberlake.** 1993. The *Aspergillus nidulans brlA* regulatory locus consists of overlapping transcription units that are individually required for conidiophore development. EMBO J. **12**:2439–2447.
43. **Rüther, U., and B. Müller-Hill.** 1983. Easy identification of cDNA clones. EMBO J. **2**:1791–1794.
44. **Sewall, T. C., C. W. Mims, and W. E. Timberlake.** 1990. *abaA* controls phialide differentiation in *Aspergillus nidulans*. Plant Cell **2**:731–739.
45. **Sikorski, R. S., and P. Hieter.** 1989. A system of shuttle vectors and yeast host strains designed for efficient manipulation of DNA in *Saccharomyces cerevisiae*. Genetics **122**:19–27.
46. **Sluka, J. P., S. J. Horvath, A. C. Glasgow, M. I. Simon, and P. B. Dervan.** 1990. Importance of minor groove contacts for recognition of DNA by the binding domain of Hin recombinase. Biochemistry **29**:6551–6561.
47. **Smale, S. T., and D. Baltimore.** 1989. The "initiator" as a transcription control element. Cell **57**:103–113.
48. **Somers, W. S., and S. E. V. Phillips.** 1992. Crystal structure of the *met* repressor-operator complex at 2.8 Å resolution reveals DNA recognition by β-strands. Nature (London) **359**:387–393.
49. **Starr, D. B., and D. K. Hawley.** 1991. TFIID binds in the minor groove of the TATA box. Cell **67**:1231–1240.
50. **St. Johnston, D., and C. Nüsslein-Volhard.** 1992. The origin of pattern and polarity in *Drosophila* embryo. Cell **68**:201–219.
51. **Stringer, M. A., R. A. Dean, T. C. Sewall, and W. E. Timberlake.** 1991. *rodletless*, a new *Aspergillus* developmental mutant induced by directed gene activation. Genes Dev. **5**:1161–1171.
52. **Timberlake, W. E.** 1990. Molecular genetics of *Aspergillus* development. Annu. Rev. Genet. **24**:5–36.
53. **Tullius, T. D., and B. A. Dombroski.** 1986. Hydroxyl radical footprinting: high resolution information about DNA-protein contacts and application to λ repressor. Proc. Natl. Acad. Sci. USA **83**:5469–5473.
54. **Ullmann, A.** 1984. One-step purification of hybrid proteins which have β-galactosidase activity. Gene **29**:27–31.
55. **White, S. W., K. Appelt, K. S. Wilson, and I. Tanaka.** 1989. A protein structural motif that bends DNA. Protein Struct. Func. Genet. **5**:281–288.
56. **Xiao, J. H., I. Davidson, H. Matthes, J.-M. Garnier, and P. Chambon.** 1991. Cloning, expression, and transcriptional properties of the human enhancer factor TEF-1. Cell **65**:551–568.
57. **Yang, C.-C., and H. A. Nash.** 1989. The interaction of *E. coli* IHF protein with its specific binding sites. Cell **57**:869–880.